OPTIMIZATION STUDIES FOR THE BEAM DYNAMIC IN THE RF LINAC OF THE ELI-NP GAMMA BEAM SYSTEM

C. Vaccarezza†, D. Alesini, M. Bellaveglia, M. Biagini, G. Di Pirro, A. Gallo, A. Ghigo, S. Guiducci, L. Sabbatini, A. Vannozzi, A. Variola, INFN-LNF, Frascati, Italy
A. Bacci, I. Drebot, D. Palmer, V. Petrillo, A. R. Rossi, L. Serafini, , INFN-MI, Milano, Italy
G. Campogiani, A. Giribono, A. Mostacci, L. Palumbo, University of Rome La Sapienza , Italy

Abstract

The ELI-NP GBS is a high spectral density and monochromatic gamma ray source based upon the inverse Compton scattering effect now under construction in Magurele. Its relevant specifications are brilliance higher than 10^{21}, 0.5% monochromaticity and a 0.2-19.5 MeV energy tunability. Strong requirements are set for the electron beam dynamic: the control of both the transverse normalized emittance and the energy spread to optimize the spectral density and guarantee the mono chromaticity of the emitted radiation. On this basis the RF Linac optimization has been performed for the designed energy range; a sensitivity analysis of the machine to possible jitters, errors and so on has been also performed, the simulations results are here presented.

INTRODUCTION

The ELI-NP GBS is an advanced gamma-ray Compton source that will be installed at the Magurele (RO) site in 2017. In the Romanian pillar of ELI (European Extreme Light Infrastructure) the gamma-ray beam is foreseen to be coupled to two 10 PW laser systems to explore the scientific potentials of such advanced infrastructure in the field of Nuclear Physics and Nuclear Photonics. This implies for the Gamma Beam System (GBS) the capability to produce a beam with extremely advanced characteristics in energy, tunability, mono-chromaticity, collimation, brilliance etc., making a steep forward jump in the available technologies in comparison to the present state of the art. In Table 1 the ELI-NP GBS source specifications are reported, on this basis the EuroGammaS* collaboration has provided a radiation source design [1] based on the Compton backscattering collision process. The frequency ν of the back-scattered photon, for the simplest case of head-on collision between the laser optical photon (frequency ν_L) and the electron is given by:

$$\nu = \nu_L \frac{2}{\frac{1}{2\gamma^2}+\frac{2h\nu}{\gamma mc^2}} \quad (1)$$

where the first term in the denominator is responsible for the typical $4\gamma^2$ scaling of Thomson Sources, while the second term in the denominator accounts for quantum effects, namely the electron recoil, and it is responsible for the correct energy and momentum conservation in the scattering reaction. The number of photons N_γ^{bw} carried by the back-scattered radiation pulse within a small angle ϑ, and the rms bandwidth $bw = \Delta\nu/\nu$ associated with it are approximately given by:

Table 1: ELI-NP Gamma Beam System Specifications

Photon energy	*MeV*	0.2-19.5
Spectral Density	*ph/sec.eV*	0.8-4·10^4
Bandwidth (rms)	*%*	≤0.5
# photons per shot within FWHM bdw.		≤2.6·10^5
# photons/sec within FWHM bdw.		≤8.3·10^8
Source rms size	*μm*	10 - 30
Source rms divergence	*μrad*	25 - 200
Peak Brilliance	(N_{ph}/sec·mm^{2}mrad^2·0.1%)	10^{20} - 10^{23}
Radiation pulse length	(rms, *psec*)	0.7 - 1.5
Linear Polarization	%	> 99
Macro rep. rate	*Hz*	100
# of pulses per macropulse		≤32
Pulse-to-pulse separation	*nsec*	16

$$N_\gamma = 7\times10^8 \frac{U_L[J]Q[pC]f\,n_{RF}}{h\nu[eV]\sigma_x^2[\mu m]}\gamma^2\vartheta^2 \quad (2)$$

in terms of the laser pulse energy U_L, the electron bunch charge Q and the laser photon energy $h\nu_L$. The rms bandwidth *bw* of the photon beam is approximately given by:

$$\frac{\Delta\nu}{\nu} \cong \sqrt{\left(\frac{\gamma^2\vartheta^2}{\sqrt{12}}+\frac{2\varepsilon_n^2}{\sigma_x^2}\right)^2+4\left(\frac{\Delta\gamma}{\gamma}\right)^2+\left(\frac{\Delta\nu_L}{\nu_L}\right)^2+\left(\frac{M^2\lambda_L}{2\pi w_0}\right)^4+\left(\frac{a_0^2/3}{1+a_0^2/2}\right)^2} \quad (3)$$

in terms of the collimation angle ϑ, the electron beam phase space density parameters (rms energy spread $\Delta\gamma/\gamma$ and transverse rms projected normalized emittance ε_n) and the laser quality parameters, rms spectral bandwidth $\Delta\nu_L/\nu_L$ and mode purity M^2. The last term represents the non-linear effects due to the laser intensity through the laser parameter $a_0 = 4.3\frac{\lambda_L}{w_0}\sqrt{\frac{U_L[J]}{\sigma_t[ps]}}$, where w_0 is the waist size at the IP and σ_t is the rms pulse length.

* http://www.e-gammas.com/
†Cristina.Vaccarezza@lnf.infn.it

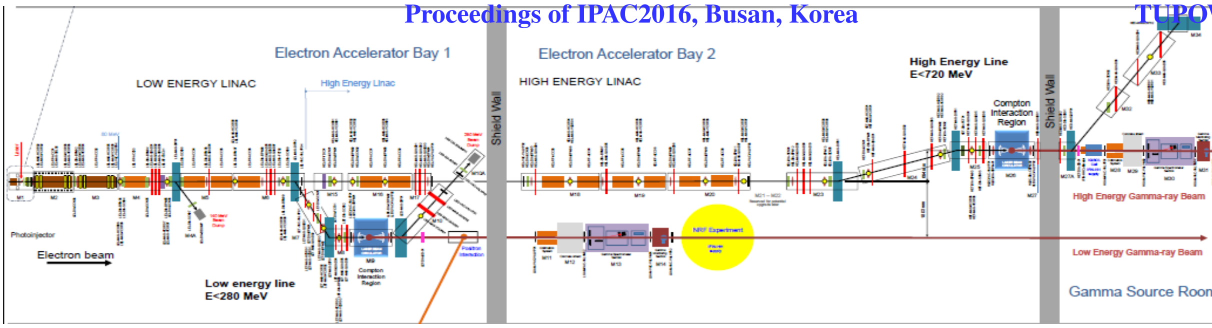

Figure 1: ELI-NP Gamma Beam System schematic layout [1].

An important basic assumption is that the collision laser is matched to the electron beam at IP, in such a way that $w_0 = 2\sigma_x$. An important figure of merit is the Spectral Density, defined as $SPD \equiv N_\gamma^{bw}/\sqrt{2\pi}h\Delta\nu$, typically expressed in units of *photons/s·eV*. Comparing Eq. 1, 2 and 3, and assuming that the dominant contributions to the bandwidth be the electron beam rms momenta (emittance and energy spread), we easily derive that the spectral density scales like:

$$SPD \propto \frac{U_L f \cdot n_{RF}}{4h\nu_L^2[eV]} \frac{Q}{\varepsilon_n^2} \frac{\vartheta^2}{\sqrt{2+\frac{\vartheta^2}{\sqrt{12}\sigma'^2_x}+2\left(\frac{\sigma_x^2 \Delta\gamma}{\varepsilon_n^2 \gamma}\right)}} \quad (4)$$

where $\sigma'_x = \frac{\varepsilon_n}{\sigma_x \gamma}$ is the rms beam diffraction angle due to emittance at IP. The expression for SPD is approximate to $O(\vartheta^2)$: fourth order terms in ϑ makes SPD saturate at a maximum at some ϑ, then slowly decreasing for larger values of ϑ. Therefore the achievable SPD scales like the phase space density of the electron beam, given by:

$$SPD \propto \frac{Q}{\varepsilon_n^2}. \quad (5)$$

Looking at the above equation the best photo-linac for such a Compton source turns out to be the one providing for the electron beam the maximum value of the parameter $\eta = Q/\varepsilon_n^2$: the hybrid scheme adopted for the Eli-NP GBS linac, where an S-band photoinjector and a C-band linac are coupled [2,3], is meant to fulfil the above requirements as described below.

THE ELI-NP GBS LINAC

The Machine Layout

The ELI-NP GBS consists in a S-band photoinjector followed by a RF Linac operated at C-band (5.7 GHz), and it is meant to deliver a high phase space density electron beam in the 75-740 MeV energy range. Two interaction points are foreseen: Low Energy (LE) at 75-320 MeV and High Energy (HE) at 320-740 as indicated in Fig. 1 where a schematic layout of the machine is reported. The repetition rate of the machine is 100 Hz, within the RF pulse, whose duration is about 450 nsec, up to 30 electron bunches will be accelerated, each one carrying 250 pC of charge, separated by 15 ns, raising the effective repetition rate of the electron bunches up to 3 kHz.

The Photoinjector

The SPARC-like photoinjector consists in a 1.6 cell RF gun equipped with a copper photocathode and an emittance compensation solenoid, followed by two S.band TW accelerating sections (SLAC-type). A gentle (compression factor <3) velocity bunching is applied in the first accelerating section, that is equipped with a 0.4 T compensating solenoid in order to inject, without emittance degradation, a short enough electron beam in the C-band following linac, reducing the final energy spread to the desired value. Three working points are have been optimized, around the reference one, to exit from the photoinjector with a final electron beam energy of E=80 ± 10 *MeV*, in order to cover the required energy range for the electron beam while preserving the beam quality. In Fig. 2 the simulations results obtained with the ASTRA [4] code, are shown from the photocathode down to the photoinjector exit for the three cases: a thermal emittance of 0.9 mm-mrad/(mm rms) is considered [5]. The considered accelerating gradient in the S-band sections ranges between E_{acc}=21-23.5 *MV/m* complying with the ELI-NP RF power distribution system. A number of 40K macroparticles has been used to simulate a 250 pC electron beam, a further optimization has been performed by means of the genetic code GIOTTO [6]. From Fig. 2 it can be seen that even at different energies the emittance and the transverse/longitudinal envelope curve are practically the same, with a very small difference from the injection in the C booster point of view.

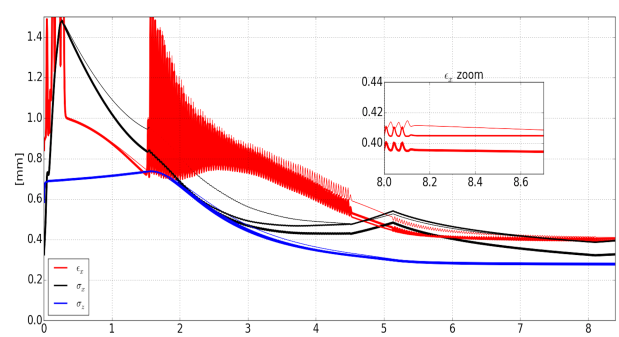

Figure 2: ASTRA output for the three reference working point, Q=250pC: evolution of emittance, transverse and longitudinal envelopes in the S-band photo-injector(red, blue and black curve), for the three foreseen final energies E=70,80,90 *MeV* (from lighter to thicker curve).

ISBN 978-3-95450-147-2

Table 2: Electron Beam Parameter List for the Different Working Points relative to the Gamma-Ray Source Energies.

γ-ray energy	**0.2**	**1.0**	**2.0**	**3.5**	**10.0**	**13.5**	**19.5**	***MeV***
e^- energy	75	165	234	312	530	605	740	*MeV*
e^- energy spread	1.14	0.86	0.82	0.80	0.45	0.43	0.48	‰
e^- rms bunch length	275	274	273	278	272	273	278	*μm*
e^- $\varepsilon_{n\,x,y}$	0.51	0.44	0.44	0.41	0.44	0.44	0.41	*mm mrad*
e^- $\beta_{x,y}$	0.16	0.43	0.43	0.55	0.71	0.71	0.95	*m*
e^- beam spot size at IP	23.5	20.0	19.6	19.4	17.3	17.3	16.2	*μm*

The Linac

Down stream the photoinjector the C-band RF- Linac is divided into two parts: in the the first four C-band, 1.8 m long, accelerating sections rise the electron beam energy up to a maximum value of E= 320 MeV, the following dogleg extracts the beam and brings it to the Low Energy Interaction Point, in the second part the electron beam energy can reach E=740 MeV, by means of the next eight C-band sections, before injecting the beam in a second dogleg that brings it to the High Energy Interaction Point. According to the gamma-ray source requirements several working points have been optimized and simulated with the Elegant code [7] and the results are summarized in Table 2. The gamma-ray source performance, have been simulated with the CAIN code [8] for the Yb-YAG laser pulse collision as described in reference [9]. A special attention has been devoted to the machine errors effects on the electron beam quality at the interaction, such as element misalignments, RF and cathode laser power jitters and so on, this study was meant to test the machine robustness, as described in detail in [10], and to provide the basis to set the machine tolerance specifications. In Table 3 the main considered errors/jitters are reported, from these values several errors affected machine-runs have been simulated with a random error distribution obtained by means of the MATLAB Latin Hypercube function. In Fig. 3 the obtained results are shown for the 10 MeV γ-ray working point, namely the electron beam spot size and energy spread at the IP, the same data are summarized in table 4.

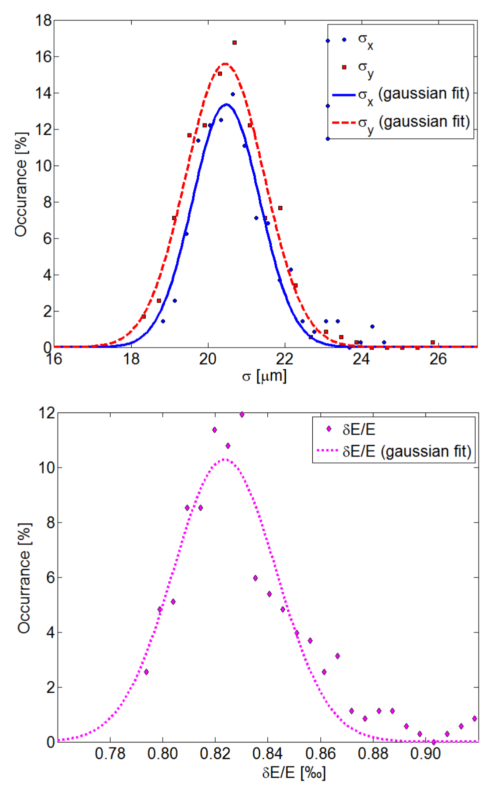

Figure 3: Electron beam spot size (above) and energy spread (below) occurrence at the Interaction Point for the 10 MeV *γ-ray* working point as obtained from a sample of 100 errors affected machine runs, with the element errors random varying within the values reported in Table 3.

Table 3: Main Error Values for Power Supplies, Magnetic Elements and Beam Position Monitors Resolution.

RF Voltage [**ΔV**] (Gun, S-C band)	±0.2 *%*
RF Phase [**ΔΦ**] (Gun, S band)	±0.2 *deg*
RF Phase [**ΔΦ**] (C band)	± 1 *deg*
Cathode Laser arrival time **[Δt]**	±200 *fs*
Cathode Laser Pointing Instabilities [**Δs**]	± 20 *μm*
Cathode Energy Fluctuation	± 5 *%*
Alignment on transverse plane [**Δ**xy]	± 70 *μm*
Beam Position Monitors Resolution	± 10 *μm*

Table 4: 10 MeV *γ-ray* WP: Main Electron Beam Parameters at IP from Simulation with and without the Described Random Insertion of Machine Errors/Jitters.

10 *MeV γ-ray WP*	No errors	With errors/jitters	
e^- energy	529.6	529.8 ± 0.5	*MeV*
e^- energy spread	0.45	0.44 ± 0.05	‰
e^- rms bunch length	272.0	272.1 ± 5.2	*μm*
e^- $\varepsilon_{n\,x,y}$	0.44	0.47 ± 0.02	*μrad*
e^- beam spot size at IP	17.3	17.8 ± 1.1	*μm*

CONCLUSIONS

The ELI-NP GBS RF Linac optimization has been presented mainly regarding the spectral density and the energy tunability requirements of the gamma-ray source. In particular, the check of the machine robustness has been addressed synthetically describing the study of the machine sensitivity to the possible errors in elements alignment, RF and cathode laser power jitters and so on. From this analysis the Linac design seems to be able to guarantee the required performances within the tolerances that have been specified for each machine element.

REFERENCES

[1] arXiv:1407.3669 [physics.acc-ph]
[2] A. Bacci *et al.*, J. Appl. Phys. 113 (2013) no.19
[3] C. Vaccarezza *et al.*, *Proc. Linac'14*, pp. 16-20
[4] K. Floettmann, ASTRA User's Manual, http://www.desy.de/~mpyflo/Astra_manual/.
[5] A. Bacci *et al .*, *Proc. IPAC' 2011*, pp. 1461-3
[7] M. Borland, "elegant: A Flexible SDDS-Compliant Code for Acc. Sim.", APS LS-287, September 2000
[6] A. Bacci, M. Rossetti Conti, V. Petrillo, "GIOTTO: A Genetic Code for Demanding Beam-Dynamics Optimizations", presented at IPAC'16, Busan, Korea, May 2016, paper WEPOY039, this conference.
[8] http://www-acc-theory_kek.jp/members/cain (1985)
[9] I. Drebot *et al.*, "Expected Gamma Spectra at ELI-NP-GBS", presented at IPAC'16, Busan, Korea, May 2016, paper TUPOW042, this conference.
[10] A. Giribono *et al.*, "6D phase space electron beam analysis and machine sensitivity studies for ELI-NP GBS", Nucl. Instr. Meth. A in press

ISBN 978-3-95450-147-2